An Injectable Oxygen and VEGF Releasing Hydrogel for Cardiac Tissue Regeneration

BEE 4530: Computer Aided Engineering | Applications to Biological Processes

May 14, 2021

Table of Contents

1.0 Executive Summary

The purpose of this study was to determine the design requirements of an injectable fibrin hydrogel as a viable tool in delivering sufficient oxygen (O_2) and vascular endothelial growth factor (VEGF) to hypoxic tissue to prevent scar tissue formation and simultaneously regenerate cardiac tissue. This study modeled changes in hydrogel size, solute concentration, and tissue damage to maximize delivery of oxygen and VEGF through an infarcted tissue region of 1.50 cm by 3.50 cm. Using COMSOL software, a 2D model of the injected hydrogel was generated to show oxygen and VEGF concentration as a function of time and space while the hydrogel deswelled following pseudo-first order kinetics.

To determine the minimum effective amount of VEGF and oxygen needed in the hydrogel to regenerate wounded cardiac tissue, different solute concentrations were tested. The hydrogel loading conditions that gave the highest average concentration over 24 hours were selected. Using this method, the hydrogel was loaded with 8×10^5 ml/m^3 O_2 and 0.8 ml/m^3 VEGF, and the therapeutic concentrations were reached at 22 hours for O_2 (2×10^{-5} ml O_2/m^3 blood) and 24 hours for VEGF (0.00137 ml VEGF/m^3). Plots of concentration vs. position were made at 4 points in time to visualize the effective diffusion distance of the hydrogel's contents and time required for delivery. VEGF diffusion had a radially symmetric distribution, while O_2 had an asymmetric diffusion pattern due to oxygen provided by the bloodstream at the inner surface of the ventricle. From the asymmetric diffusion distribution, the location of optimal injection in the myocardial wall was concluded to be ⅓ of the distance from the heart surface to the ventricle. A sensitivity analysis was also done for all the parameters, and the final concentration of oxygen and VEGF in the damaged tissue was found to be most sensitive to hydrogel radius, which impacted the design recommendations. Determination of the proper concentration of dissolved substituents, hydrogel size, and diffusion time will assist surgeons, bioengineers, and material scientists in designing a viable injectable hydrogel.

Key Words: Hydrogel, Cardiac Tissue, Infarction, VEGF, Drug Delivery, Oxygen Release

2.0 Introduction

2.1 Background

Heart disease is the leading cause of death in the United States, and coronary artery disease is the most common form of heart disease [1]. In the United States, approximately 800,000 people have a heart attack every year [1]. A heart attack, also known as a myocardial infarction, occurs when portions of the heart do not receive enough blood. Blood transports oxygen to the tissues to maintain cellular functions. Without oxygen, tissues can only survive a number of days, so most treatments today aim to restore blood flow to the heart. After a heart attack, remaining live

cardiomyocytes regenerate healthy tissue, but dead heart cells form scar tissue instead. Scar tissue takes approximately 3 weeks to form and is more rigid than normal tissue, which reduces the heart's pumping strength and efficiency [2]. Thus, people who form more cardiac scar tissue after a heart attack are at a higher risk of experiencing severe heart issues, such as arrhythmia, coronary artery disease, and in severe cases, heart failure [3].

2.2 Literature Review

A possible strategy to prevent scar tissue formation is to introduce regenerative materials as soon as possible. In a study by Gholipourmalekabadi et al., several types of hydrogels and their structures were investigated for their viability in restoring cardiac tissue [4]. The study introduced the idea of an oxygen-delivering hydrogel to heal and regenerate the dying, hypoxic tissue. Oxygen is released via a PVP/H_2O_2/catalase complex, which forms a core shell microsphere and is encapsulated in the fibrin hydrogel. Oxygen is released from this complex at a constant rate [4]. Vascular endothelial growth factors (VEGF), which promotes the formation of new blood vessels, can also be delivered from a hydrogel to damaged myocardial tissue. VEGF is a natural glycoprotein that improves cell survivability and proliferation by stimulating glucose uptake and increasing vascular permeability [5]. After myocardial infarction, VEGF in the wounded tissue is quickly depleted [6]. Zhu et al has shown that VEGF-releasing hydrogels improve cardiac function in rats who have suffered a myocardial infarction [7]. Although research has primarily been limited to animal studies, this study used properties of the human heart ventricle.

Prabhat et al. explored the effect of supplemental oxygen on damaged cardiac tissue [8]. By treating several samples of tissue with varying concentrations of oxygen, they discovered that delivering a 95% oxygen (5% CO_2) mixture was most effective at rejuvenation. Peak oxygen concentrations were observed around 12-30 minutes after delivery. Although the study determined the amount of supplemental oxygen needed to regenerate a tissue sample, the amount of tissue healed was not measured. To improve this study's medical relevance, the simulation in this paper quantifies the amount of healed tissue using oxygen delivery profiles and measurement of peak oxygen concentrations. Obtaining this information will improve the development and design of oxygen-releasing hydrogels.

Another area that has not been well-researched is to what extent a hydrogel's deswelling rate affects drug release rate. A hydrogel initially swells upon injection, then deswells and degrades over time due to solvent composition, pH, temperature, or solute concentration. In this paper, the deswelling is represented as a moving boundary condition in the simulation. In Zhu et al., the swelling ratios for different polymer structures were outlined, including fibrin [6]. The study explained how contents of a filled hydrogel, such as oxygen and VEGF, are "locked" inside the hydrogel prior to delivery. Fibrin, a natural polymer, has been used extensively in cardiac tissue applications for its elastic properties, an extremely important attribute in an environment that is constantly contracting and expanding. Due to its elasticity and wide availability of research on its

diffusive properties, fibrin was chosen as the hydrogel material for this study. By investigating the viability of an oxygen and VEGF-releasing fibrin hydrogel, this study adds to current research on injectable polymeric hydrogels for the delivery of therapeutic agents.

2.3 Problem Statement

The major limitation in current research is the transformation from qualitative to quantitative results. Previous studies concluded that fibrin was a good material for oxygen diffusion, but the exact diffusion distances and times are unknown since these values are difficult to measure in live animal studies [7]. Therefore, this study models the ventricle in a controlled setting using COMSOL. The results from the model will be used to determine the optimal concentrations of oxygen and VEGF needed in the hydrogel to treat a sample of infarcted tissue, the distance each species will travel through the tissue, and the duration of treatment. These results will provide quantitative characteristics of the treatment, i.e. the number of injections needed to treat an infarcted region and the distance between injection sites.

2.4 Design Objectives

This study aimed to characterize oxygen and VEGF mass transfer in ventricle tissue beyond what previous experiments examined. Some major limitations in current studies are the lack of data for diffusive distances and treatment duration. This study focused primarily on modeling a situation in which those factors could be quantified. Specifically, there were three key objectives that this experiment targeted:

1. Determine time since injection of the hydrogel to deliver an effective amount of VEGF and oxygen to the entire wounded region.
2. Determine the initial concentration of oxygen and VEGF needed in the hydrogel to deliver a sufficient amount of oxygen and VEGF to the entire wounded region.
3. Determine the distance that therapeutic levels of oxygen and VEGF will reach within the myocardial tissue.

Accurately quantifying these three characteristics of oxygen and VEGF delivery will increase the current level of understanding of drug delivery. In doing so, this experiment will build upon the aforementioned limitations and allow for future research on drug therapies for acute myocardial infarction.

3.0 Methods

3.1 Schematic

A hydrogel loaded with two therapeutic agents was injected into the damaged myocardial tissue surrounding the ventricle, where it gelated into a sphere. The VEGF and oxygen uniformly

diffused out of the spherical hydrogel, allowing for the simplification to a 2D, axisymmetric geometry (outlined by the green box in Figure 1c). Half of the hydrogel was modeled and represented as a semi-circle. Mass transfer of the VEGF and oxygen occurred only in the r direction. A convection boundary was included at the top boundary to represent the bloodstream supplying a bulk flow of oxygen to the cardiac tissue. Over time, the VEGF and oxygen diffused throughout the entire wounded area and into the surrounding healthy tissue. At the far end of the healthy tissue, there was zero diffusive flux of oxygen and VEGF since the tissue fully absorbed both species by this point. The following diagram depicts the geometry of this study, beginning with a cross section of the ventricle (Figure 1a). Figure 1b shows the injection site and is roughly the same orientation as Figure 1c, which is the simplified schematic of the computation. Note that this study only measured oxygen and VEGF concentrations inside the green box region, since the axisymmetric condition assumed the other half was identical. Finally, Figures 1d and 1e show the shrinking of the hydrogel over time as deswelling occurs.

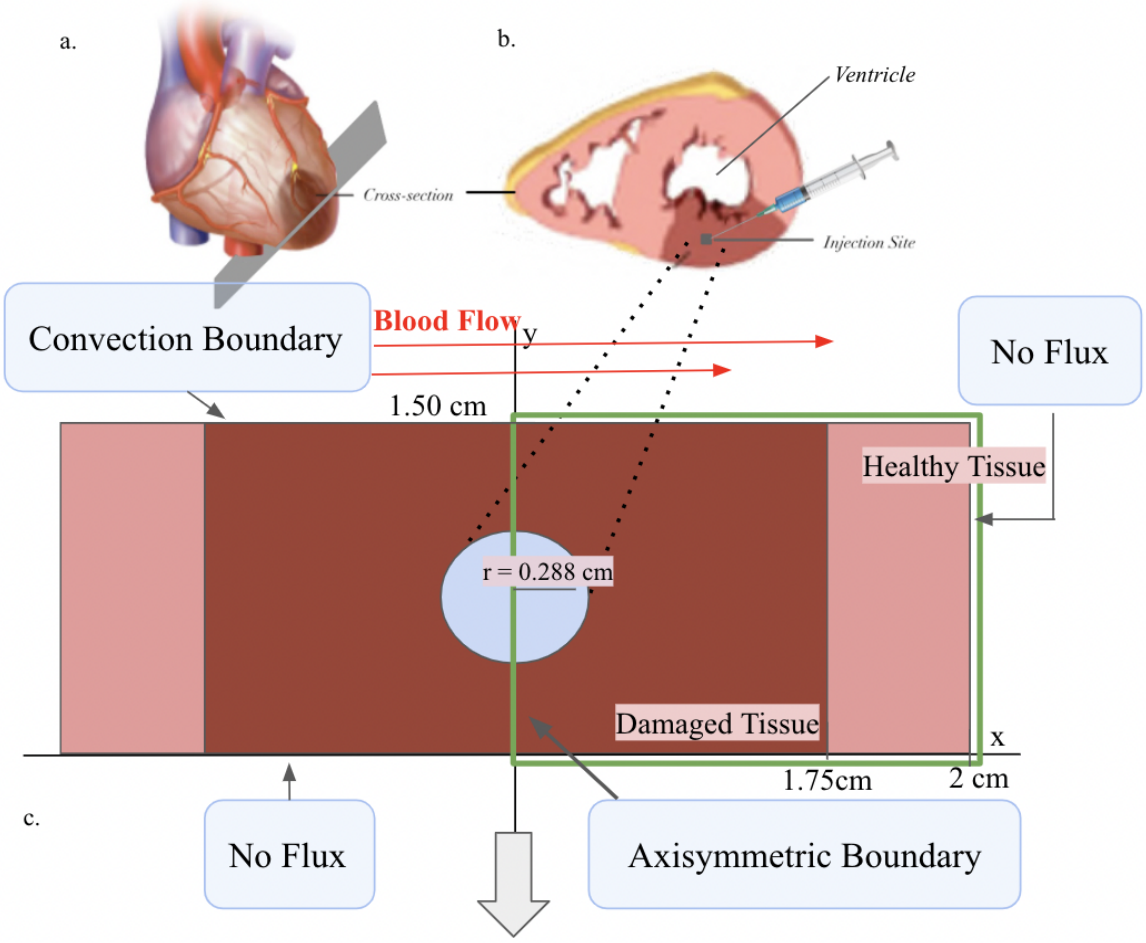

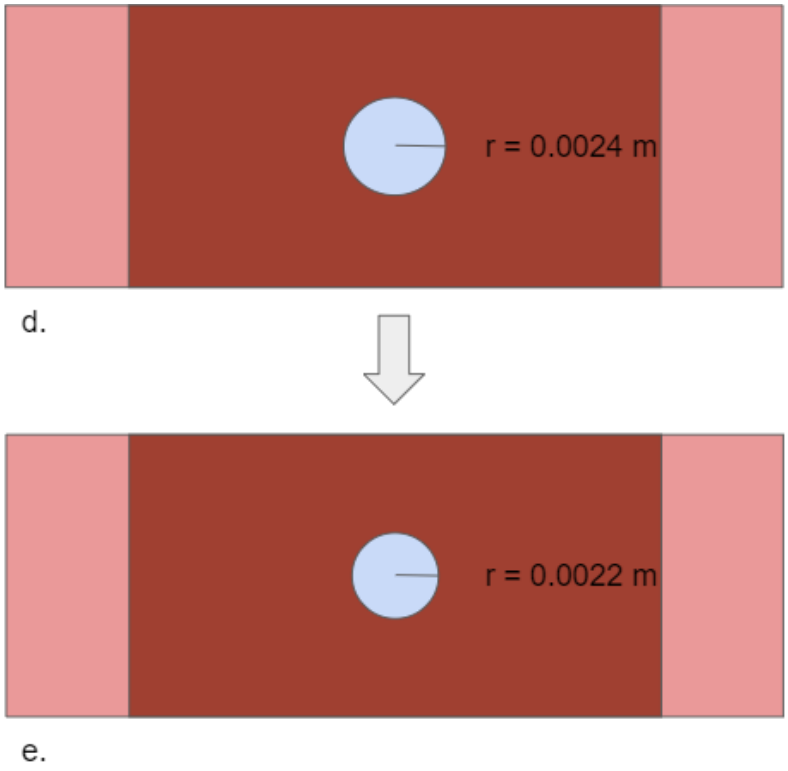

Fig. 1. Geometry of Hydrogel Model. a) Depiction of a heart with damaged myocardial tissue after a heart attack. b) Cross-sectional area of interest within the heart with the hydrogel being injected into the damaged tissue. © 2007 Terese Winslow LLC c) Schematic with boundary conditions and simplified geometry of process: hydrogel modeled as a sphere and surrounding tissue modeled as a rectangular slab. d and e) Hydrogel shrinking over time.

This schematic shows the injection process and changing geometry of the hydrogel within the myocardial wall. Figures 1a and 1b give cross-sections of the wounded heart after myocardial infarction. Figure 1c shows the initial state of the system that was modeled, which was set at a time after absorption of water into the porous, hydrophilic hydrogel matrix has allowed the hydrogel to fully swell. Time 0 was the time at which the hydrogel began to deswell, or shrink, as the concentration gradient of oxygen and VEGF drove the substances out. In Figures 1d and 1e, the hydrogel shrinks according to pseudo first-order kinetics.

3.2 Governing Equations

Consistent with the problem formulation, there was no bulk fluid flow or heat diffusion through the domain. The only physical process occurring was mass diffusion. Equation (1) shows the mass diffusion of substance (A) through a solid (B) in cylindrical coordinates.

$$D_{AB}\left[\frac{1}{r}\frac{\partial}{\partial r}\left(r\frac{\partial c_A}{\partial r}\right) + \frac{1}{r^2}\frac{\partial^2 c_A}{\partial \theta^2} + \frac{\partial^2 c_A}{\partial z^2}\right] + r_A = \frac{\partial c_A}{\partial t} \quad (1)$$

In equation (1), D_{AB} represents the diffusivity of substance (A) through a solid (B) and r represents the radius in a cylindrical coordinate system. The two directions in which diffusion occurred were r and z. The reaction term was represented by r_A, and $\frac{\partial c_A}{\partial t}$ was the change in concentration over time.

Equation (1) was used to model the mass diffusion of oxygen and VEGF through the hydrogel and myocardial tissue. Mass diffusion only occurred in the radial direction. Since the problem was modeled in 2D, only diffusion in the r and z directions of the governing equations were considered, while the θ term was eliminated.

$$D_{O_2-H}\left[\frac{1}{r}\frac{\partial}{\partial r}\left(r\ \frac{\partial c_{O_2}}{\partial r}\right) + \frac{\partial^2 c_{O_2}}{\partial z^2}\right] = \frac{\partial c_{O_2}}{\partial t} \quad (2)$$

D_{O_2-H} was defined as the diffusion constant for oxygen through the hydrogel and c_{O_2} represented the concentration of oxygen. There was no chemical reaction of oxygen in the hydrogel, so the reaction term was eliminated for oxygen diffusion. Diffusion was not at steady state, so the transient term ($\frac{\partial c_{O_2}}{\partial t}$) was retained in equation (2), which describes diffusion of oxygen (O_2) through the hydrogel (H).

$$D_{V-H}\left[\frac{1}{r}\frac{\partial}{\partial r}\left(r\ \frac{\partial c_V}{\partial r}\right) + \frac{\partial^2 c_V}{\partial z^2}\right)] = \frac{\partial c_V}{\partial t} \quad (3)$$

Equation (3) describes diffusion of VEGF through the hydrogel; the diffusion constant was defined as D_{V-H}, and c_V was the concentration of VEGF. Similarly, there was no degradation reaction of VEGF occurring in this region.

Both oxygen and VEGF diffused across the hydrogel and tissue interface. Within the tissue region, the diffusivity constant for oxygen was defined as D_{O_2-T}, and the transient term was included. This is shown in Equation (4) for diffusion of oxygen (O_2) through the damaged myocardial tissue (T).

$$D_{O_2-T}\left[\left[\frac{1}{r}\frac{\partial}{\partial r}\left(r\ \frac{\partial c_{O_2}}{\partial r}\right) + \frac{\partial^2 c_{O_2}}{\partial z^2}\right] + r_{O_2}\right|_{t<30} = \frac{\partial c_{O_2}}{\partial t} \quad (4)$$

Since oxygen was being consumed by the cells in the surrounding tissue, the reaction term was also included in the r_{O_2} term. The reaction was only present for the first 30 minutes since, afterwards, the blood vessels were able to reintroduce oxygen to the heart.

Equation (5) represents the diffusion of VEGF (V) through the damaged myocardial tissue (T) and is shown below.

$$D_{V-T}[\frac{1}{r}\frac{\partial}{\partial r}(r\ \frac{\partial c_V}{\partial r}) + \frac{\partial^2 c_V}{\partial z^2})] + r_V|_{t<30} = \frac{\partial c_v}{\partial t} \quad (5)$$

The diffusivity constant for the diffusion of VEGF through the myocardial tissue was D_{V-T}. The VEGF was being integrated into the surrounding myocardial tissue as it diffused through the domain; however, the VEGF will degrade over time and has a half life of approximately 30 minutes. The consumption rate was therefore included in the r_v term, which only applied in the tissue region at times less than 30 mins.

Equation (6) represents diffusion of oxygen (O_2) through the healthy myocardial tissue (T). Equation (7) represents the diffusion of VEGF (V) through the healthy myocardial tissue (T).

$$D_{O_2-T}[[\frac{1}{r}\frac{\partial}{\partial r}(r\ \frac{\partial c_{O_2}}{\partial r}) + \frac{\partial^2 c_{O_2}}{\partial z^2}] = \frac{\partial c_{O_2}}{\partial t} \quad (6)$$

$$D_{V-T}[\frac{1}{r}\frac{\partial}{\partial r}(r\ \frac{\partial c_V}{\partial r}) + \frac{\partial^2 c_V}{\partial z^2})] = \frac{\partial c_v}{\partial t} \quad (7)$$

The diffusivity constant for the diffusion of VEGF and oxygen through the healthy myocardial tissue was assumed to be the same as for the damaged tissue (Equation 6 and 7). There should be no net consumption of oxygen in healthy tissue, so there was no reaction rate in this region. VEGF was only present in very minute amounts in healthy tissue, and therefore it can be assumed that there was little degradation. This allowed for the approximation of the reaction rate to be zero.

3.3 Boundary Conditions

In order to solve the governing equations, the following boundary conditions were defined: There was zero flux of oxygen and VEGF across the vertical line of symmetry at *r* equals 0 (as defined by the green box in Figure 1c) due to axisymmetry in both the hydrogel and the tissue. The axisymmetric boundary conditions were represented by Equations (8), (9), (10), and (11).

$$\text{Oxygen } (O_2): -D_{O_2-H}\frac{dc_{O_2}}{dt}|_{r=0;\ 0.0046\ m<\ z<0.0104\ m} = 0 \quad (8)$$

$$-D_{O_2-T}\frac{dc_{O_2}}{dt}|_{r=0;\ 0<z<0.00462\ m\ and\ \ 0.0104\ m<z<0.015\ m} = 0 \quad (9)$$

$$\text{VEGF (V)}: -D_{V-H}\frac{dc_V}{dt}\Big|_{r=0;\ 0.0046\,m<\ z<0.0104\,m} = 0 \tag{10}$$

$$-D_{V-T}\frac{dc_V}{dt}\Big|_{r=0;\ 0<z<0.00462\,m\ and\ \ 0.0104\,m<z<0.015\,m} = 0 \tag{11}$$

There was convection at the interface between the myocardial tissue and the blood within the ventricle of the heart due to blood flow (top edge of the domain). The velocity of the blood relative to the tissue was measured to be around 15 inches per second, or 381 mm per second [9]. Due to the high velocity of the blood flow in the heart, it was assumed that the convection coefficient *h* is extremely large. Thus, the boundary condition at the top edge of the domain was constant concentration. Using these assumptions, Equation (12) was simplified to Equation (13), and the concentration of oxygen in the tissue at the top edge is equal to the concentration of oxygen in the blood. Similarly, Equation (14) was simplified to Equation (15), as there is no VEGF present in the blood flow.

$$\text{Oxygen } (O_2): \tag{12}$$

$$-D_{O_2-T}\frac{dc_{O_2}}{dt}\Big|_{z=0.015m,\,r} = h_m\left(c_{O_2}^{\ fluid}\Big|_{z=0.015m} - c_{O_2}^{\ fluid}\Big|_{z=\infty}\right);\ h_m \to \infty$$

$$c_{O_2-tissue}\Big|_{z=0.015\,m} = c_{O_2-blood} \tag{13}$$

$$\text{VEGF (V)}: -D_{V-T}\frac{dc_V}{dt}\Big|_{z=0.015m,\,r} = h_m\left(c_V^{\ fluid}\Big|_{z=0.015m} - c_V^{\ fluid}\Big|_{z=\infty}\right);\ h_m \to \infty \tag{14}$$

$$c_{V-tissue}\Big|_{z=0.015\,m} = c_{V-blood} = 0 \tag{15}$$

The outside edge of the heart tissue bordered the pericardium. Therefore, there was zero flux in both diffusive species at the interface between the myocardial tissue and the pericardium (bottom edge of the domain). Equation (16) represents the zero flux of oxygen at the interface between the myocardial tissue and the pericardium. Equation (17) represents the zero flux of VEGF.

$$Oxygen\ (O2):\ \ -D_O\frac{dc_{O_2}}{dt}\Big|_{z=0,\,r} = 0 \tag{16}$$

$$\text{VEGF (V)}: -D_V \frac{dc_V}{dt}\Big|_{z=0,r} = 0 \tag{17}$$

There was zero flux in all diffusive species in the healthy tissue at a distance far away from the hydrogel (right edge of the domain) as seen in Equation (18) for diffusion of oxygen at a far distance and Equation (19) for diffusion of VEGF.

$$\text{Oxygen } (O_2): -D_{O_2-T} \frac{dc_{O_2}}{dt}\Big|_{r=0.02\,m,z} = 0 \tag{18}$$

$$\text{VEGF (V)}: -D_{V-T} \frac{dc_V}{dt}\Big|_{r=0.02\,m,z} = 0 \tag{19}$$

Finally, the hydrogel deswelled over time as oxygen and VEGF were released. Variations in pH, ionic strength, and solvent concentration may have caused the reduction in hydrogel volume. To represent this volume change, the radius of the hydrogel changed with time based on Equation (20). The deswelling rate can be approximated by the exponential decay function, Equation (21). R_i was the radius of the hydrogel at time t equals 0 and k was a rate constant. (See Appendix 7.C for the derivation of the normal mesh velocity, *v*.)

$$\frac{dr}{dt} \cdot n = v \tag{20}$$

$$v = \frac{-R_i \cdot k}{3} \cdot e^{\frac{-kt}{3}} \tag{21}$$

3.4 Initial Conditions

The governing equations included the transient term and initial conditions since the process being modeled was not at steady-state. The initial concentrations of oxygen and VEGF in the hydrogel were equal to$c_{O_2 i}$ and c_{Vi}, respectively, as defined in Equation (22) and (23).

$$c_{O_2}(t = 0)|_{hydrogel} = c_{O_2 i} \tag{22}$$

$$c_V(t = 0)|_{hydrogel} = c_{Vi} \tag{23}$$

The initial concentrations of oxygen in healthy and damaged tissues were equal to $c_{O_2 HTi}$and $c_{O_2 DTi}$, respectively, as defined in Equations (24) and (25). The initial concentration of VEGF in the entire

myocardial tissue domain was equal to 0, as defined in Equation (26). (The myocardial tissue consists of the region between $0 < r < 0.02\ m$ and excludes the hydrogel region defined above.)

$$c_{O_2}(t = 0)|_{damaged\ myocardial\ tissue} = c_{O_2HTi} \tag{24}$$

$$c_{O_2}(t = 0)|_{healthy\ myocardial\ tissue} = c_{O_2DTi} \tag{25}$$

$$c_V(t = 0)|_{myocardial\ tissue} = 0 \tag{26}$$

These governing equations, boundary conditions, and initial conditions were implemented to create the model to realistically represent the process of mass diffusion within the tissue of the heart.

4.0 Results and Discussion

4.1 Mesh Convergence

A mesh convergence analysis was performed for both diffusive species, O_2 and VEGF. A specific cut point was chosen within the domain where the concentration of species was sensitive to time. This point was chosen as (0.001, 0.004), as shown in the mesh of the 2D diagram below (Fig 2). The point was chosen because it is in a region heavily influenced by the diffusion from the hydrogel and the convective boundary condition.

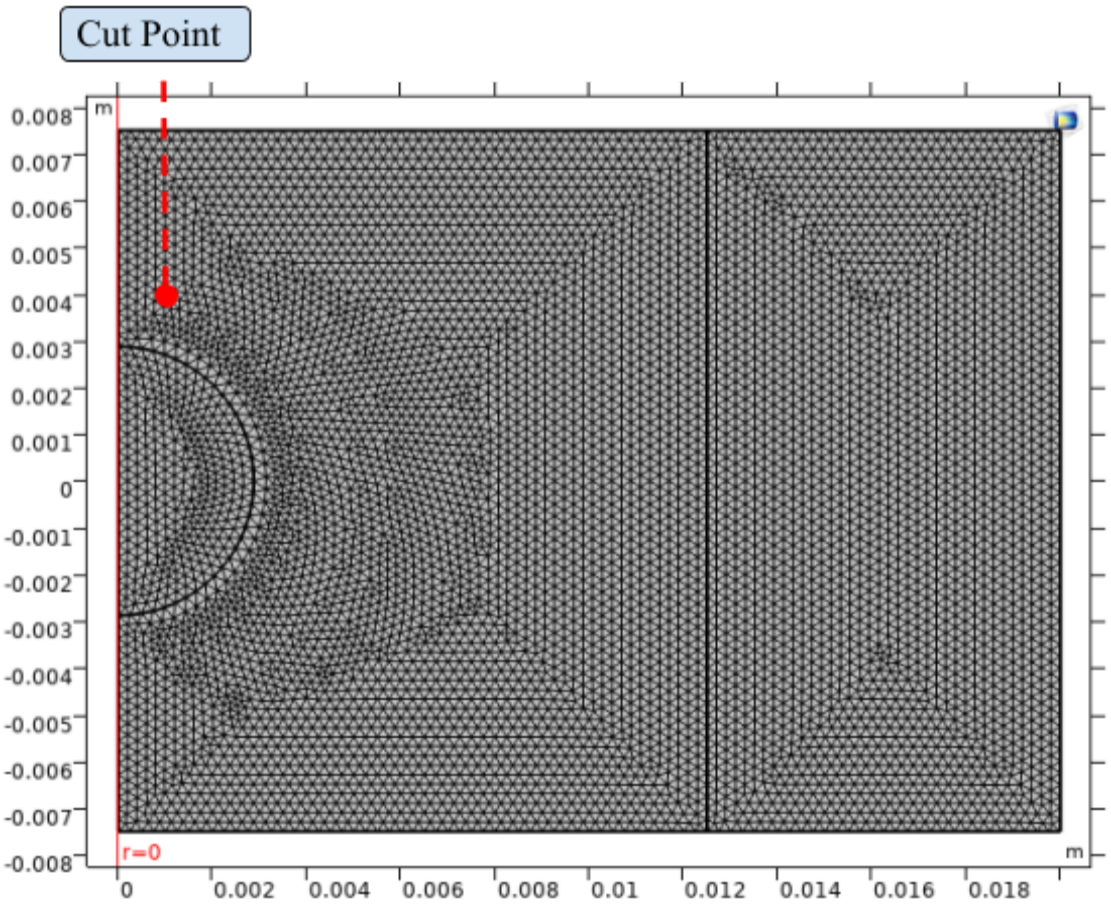

Fig. 2. Geometry in COMSOL with Mesh. The mesh contains 12735 domain elements. The cut point chosen for the mesh convergence analysis is shown by the red dot in the diagram.

The computation was run several times, each with a different mesh size ranging from extremely coarse (47 domain elements) to extremely fine (35061 domain elements), and the concentration of O_2 and VEGF at t=30 mins was extracted from the cut point. Figure 3 shows the convergence of the concentration values as the number of domain elements was increased.

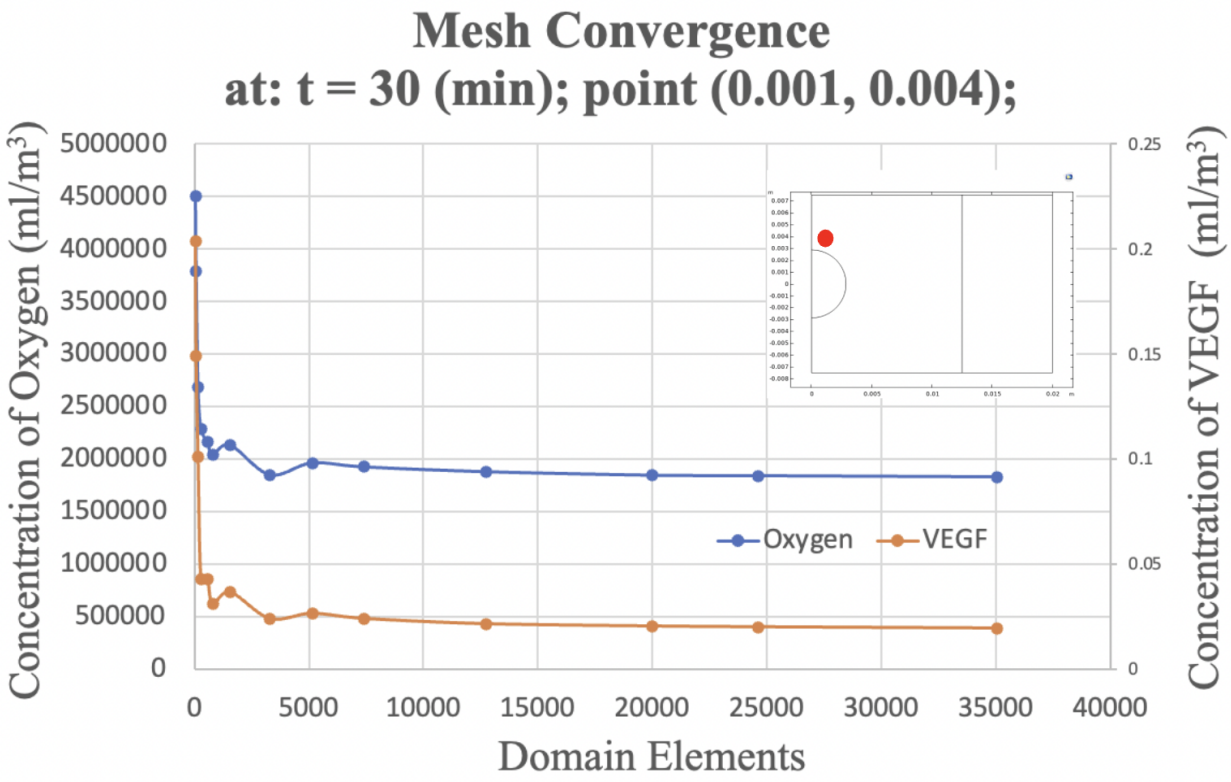

Fig. 3. Mesh convergence analysis of O_2 and VEGF. The concentrations illustrate that the plateau occurs near 12735 domain elements. An image of the geometry with the cutpoint was also included.

For both species, convergence occurred at 12735 domain elements, which marks the start of the plateau region in Figure 3. Selecting 12735 domain elements as the mesh size optimized the accuracy of the results obtained and minimized unnecessary computation time.

4.2 Time Step Convergence

A time step convergence analysis was performed for both diffusive species, O_2 and VEGF at the cut point (0.001, 0.004) for concentration at 12 hours. The computation was run several times, each at a different time step. The time step converged at 2 hours, as seen in Figure 4.

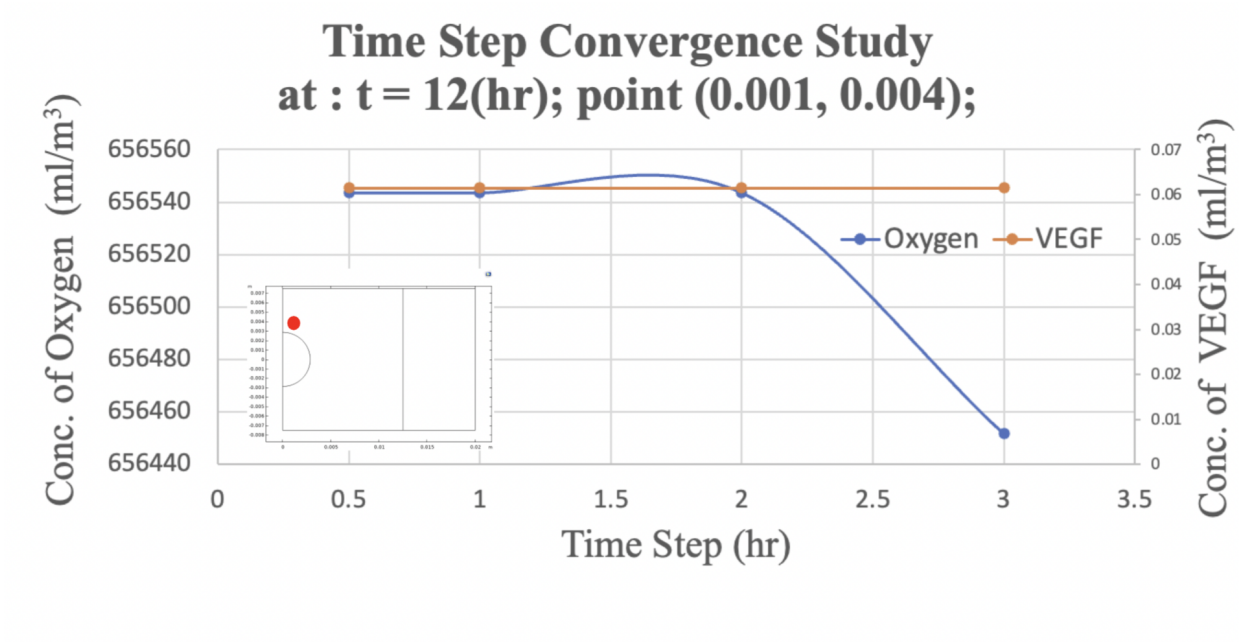

Fig. 4. Time step convergence. The analysis occurred at a cut point (0.001, 0.004) at 12 hours for O_2 and VEGF concentration. The plateau for oxygen begins around a time step of 2 hours, while the plateau for VEGF starts at 3 hours. An image of the geometry with the cutpoint was also included.

After 2 hours, both oxygen and VEGF concentrations in the damaged tissue were independent of a decreasing time step. For convenience and greater accuracy, this simulation used a time step of 1 hour.

4.3 Model Description

The previously defined conditions were used to model a hydrogel with controlled release of oxygen and VEGF. As seen in Figure 5, the hydrogel shrinks in volume over the course of 24 hours from a radius of 0.0028 m (at time zero) to a radius of 0.0022 m.

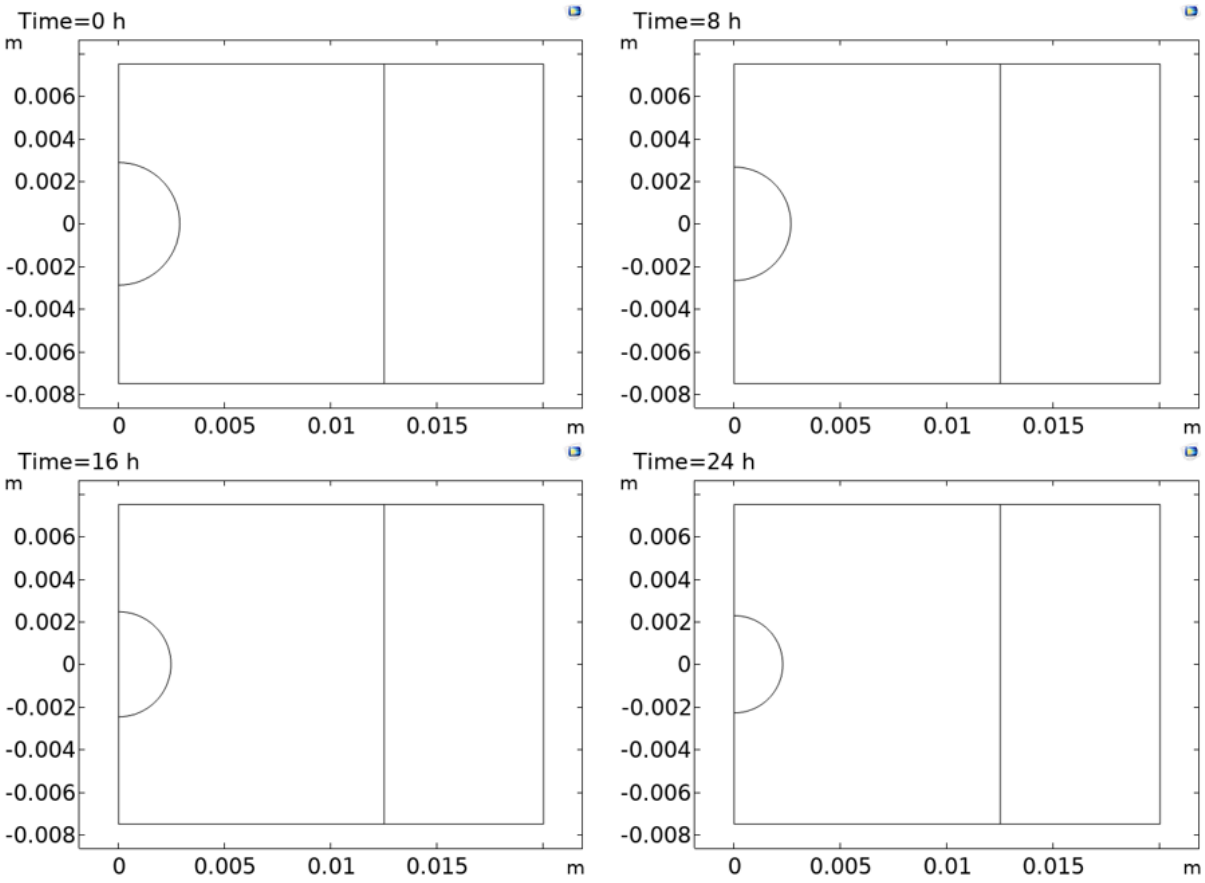

Fig. 5. Hydrogel Shrinking. The COMSOL model shows the hydrogel shrinking over the course of 24 hours. The initial radius is 0.0028 m, and the final radius at 24 hours is 0.0022 m.

The hydrogel halved in volume within 24 hours. Volume reduction increased the diffusion rate due to O2 and VEGF becoming more concentrated in the hydrogel as it shrunk, thereby increasing the concentration gradient (see Fig 6 and 7). The VEGF diffused symmetrically out of the hydrogel as seen in Figure 6. This was in agreement with expectations, since the boundary conditions were all symmetric. The VEGF also reached all areas of the damaged tissue by 24 hours.

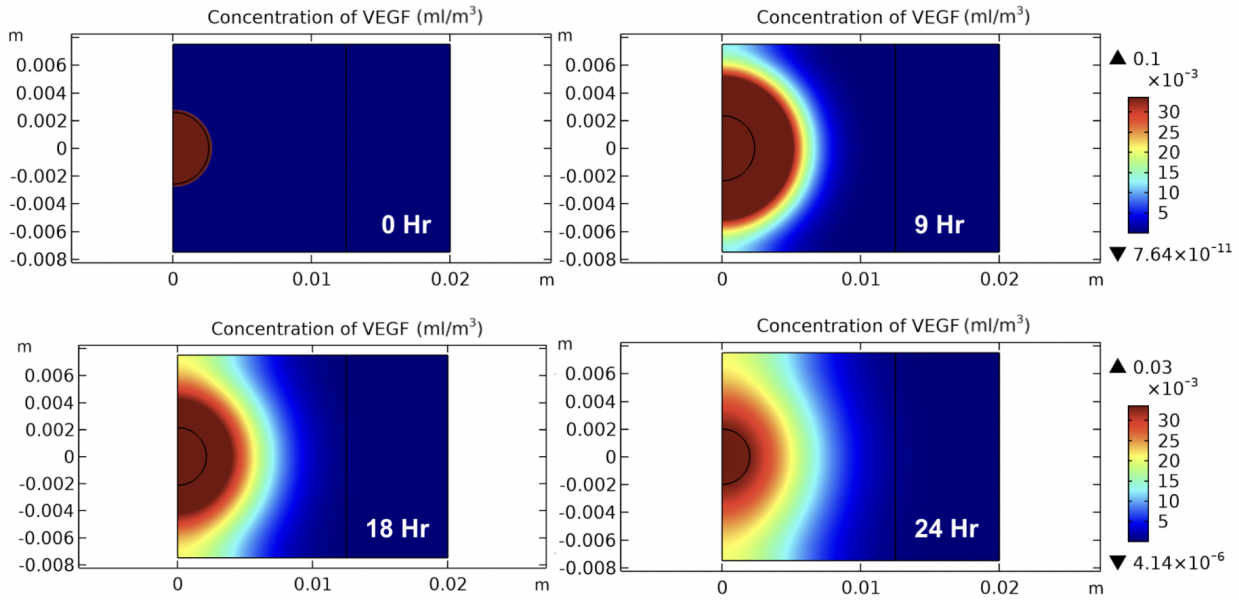

Fig 6. Progression of VEGF diffusion at times 0, 9, 18, and 24 hours. VEGF diffuses symmetrically from the hydrogel to the entire damaged tissue region in 24 hours as the hydrogel gradually deswells.

Oxygen diffusion from the hydrogel was also measured, as seen in Fig 7. The oxygen diffusion process was asymmetric because oxygen was not only supplied by the hydrogel, but also from a convective boundary condition at the top of the damaged tissue. After approximately three hours, the convective boundary became the major supplier of oxygen to the tissue. At 22 hours, the oxygen from both these sources had reached the therapeutic level in the entire infarcted tissue region.

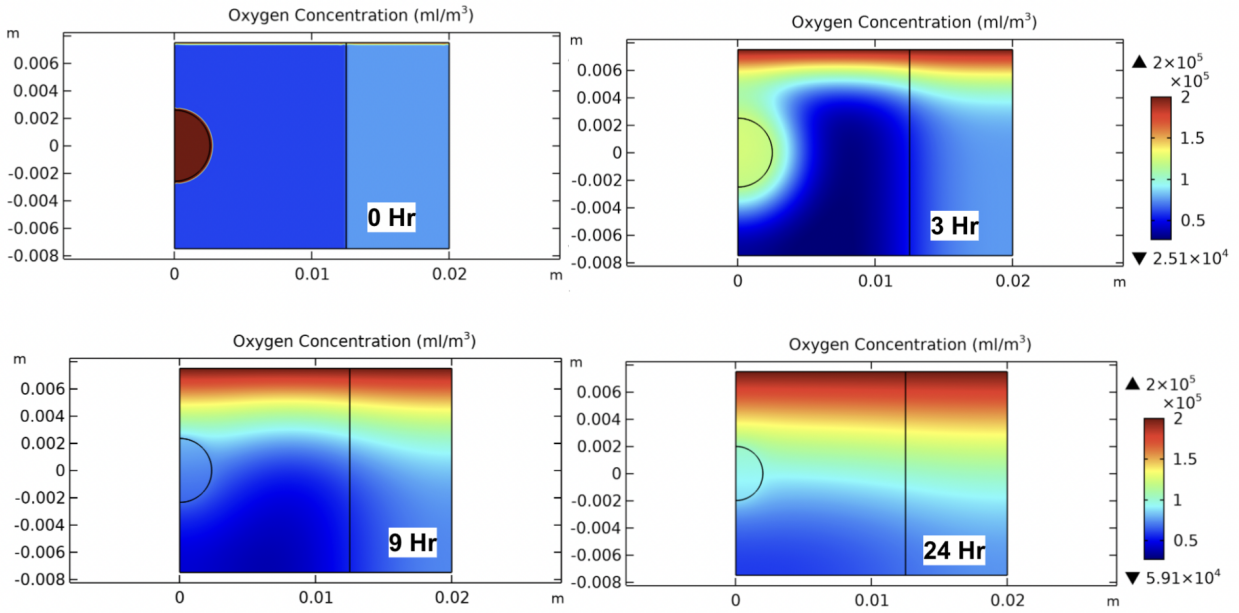

Fig 7. Progression of Oxygen diffusion at times 0, 3, 9, and 24 hours. Oxygen diffuses into the hypoxic region of the myocardium from the deswelling hydrogen and from the a natural convection of oxygen-filled blood from the face of the heart facing the ventricular blood flow.

The model depicted the expected diffusion of oxygen and VEGF from a shrinking hydrogel into the hypoxic region of the myocardium (Fig 6 and 7). Largely aided by the additional supply from the convective boundary condition, oxygen diffused throughout the tissue at a much faster rate than VEGF.

4.4 Model Validation

Validation of the model's release of oxygen was performed by plotting the cumulative oxygen release as a percentage of the initial concentration in the hydrogel as a function of time. Experimental data for the comparison was obtained from Gupta et al [10]. In this study, the researchers measured drug release from an ABC triblock polymer that incorporated mechanisms for reactive oxygen species (ROS) triggered degradation [10]. The triblock polymer (PPS-b-PDMA-b-PNIPAAM) formed physically-crosslinked hydrogels, and as the reactive oxygen species degraded in an aqueous environment, oxygen was released from the hydrogel with the drug. The experiment was conducted at 37℃ for 64 hours. The diffusivity constant of oxygen through a related hydrogel was 3.7×10^{-14} m^2/s at 15ºC by Yargi et al. [11], while the diffusivity constant of oxygen through the surrounding tissue was found to be 1×10^{-10} m^2/s by McMurtrey [12]. These values were used in the model for validation. Figure 8 shows a comparison of this experiment's cumulative release of oxygen from the hydrogel in the model vs Gupta et al [10]. Both experiments begin at 0% released at time 0, and reach a plateau region at approximately 85% after 65 hours.

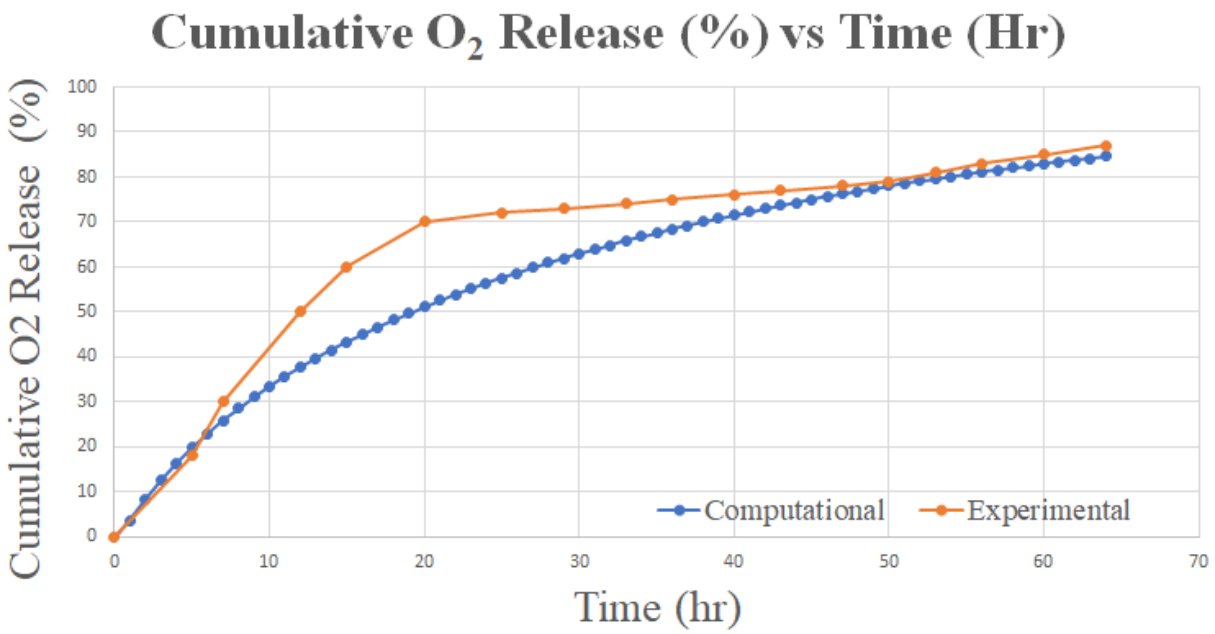

Fig 8. Cumulative O_2 release from hydrogel. Both computational and experimental data released up to ~85% after 64 hours. The computational data showed a slower initial release rate than the experimental data, though the experimental data plateaued after 20 hours.

However, as seen in Figure 8, the cumulative O_2 release from the hydrogel was slightly different from the experimental results. Not only did both datasets approach different cumulative release percentages of O_2 up until 25 hours, but there was also a significant difference in the rate of release during the 10-40 hour period. The experimental curve used from Gupta et al. had a lower average release rate between 0 and 20 hours [10]. The experimental release rate diverged from the computation until 20 hours, which is when the release rate began to plateau. Errors in the computational model could have arisen from the difference in size of the hydrogels used in each case. The O_2 release was dependent on the size of the hydrogel spheres, but the researchers did not specify the size of the hydrogel particles used in the experiment. Lastly, the computation used a diffusion coefficient measured at 40ºC, while the experiment was run at an ambient temperature of 37ºC.

Next, the experimental data for the VEGF release rate was obtained from Ouyang et al [13]. In this paper, the researchers measured matrix-metalloproteinase (MMP) dependent VEGF release from a PEG hydrogel. When measuring the release rate, the cumulative release percentage was held constant at 40% between 0 to 72 hours, before allowing for the release of VEGF at 72 hours [13]. Only the cumulative release from 72 hours to 144 hours was considered in this model. The cumulative release at 72 hours was set to 0%. The diffusivity value of VEGF in the PEG hydrogel, 80 μm^2/s, was obtained from Limasale et al and used for validation [14]. Figure 9 shows the

computed cumulative release of VEGF compared to the experimental release rate obtained from Ouyang et al [13].

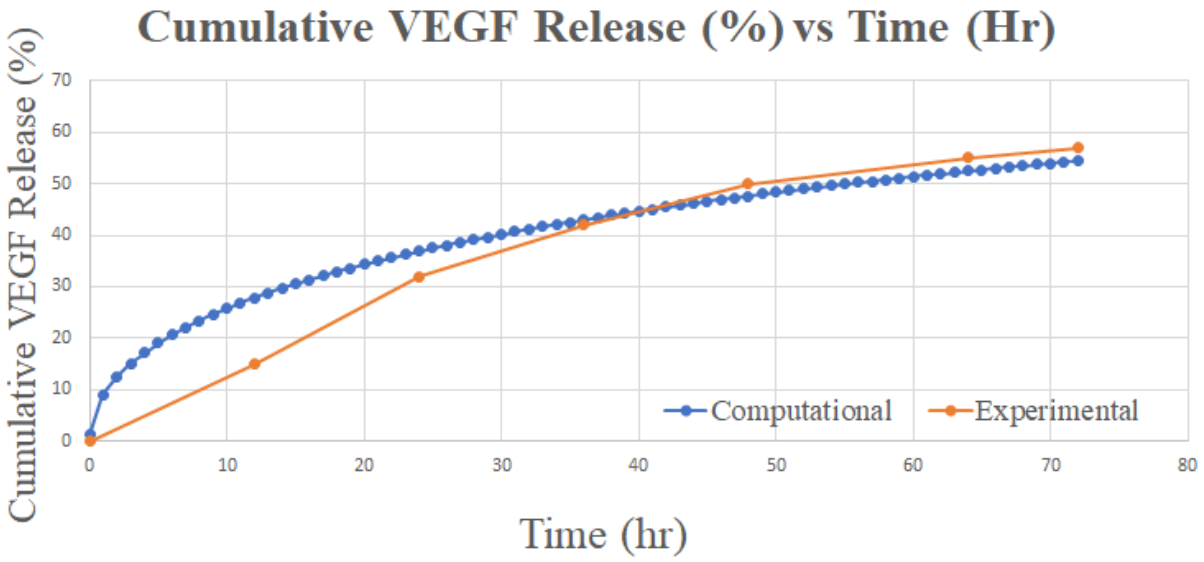

Fig 9. Cumulative VEGF Release vs Time. Both datasets converge around 72 hrs to a release of 60% and have the most similar VEGF release percentages after 35 hours.

As seen in Figure 9, the computed cumulative release of VEGF overestimates the release percent of VEGF for the first 30 hours compared to the experimental release. This is likely due to an error in the computational assumptions. At time 0, the initial concentration of VEGF within the hydrogel is less than the input parameter of initial concentration, leading to a 12% cumulative release at time 0. This may be due to an inaccurate estimation of the hydrogel size in the model since the hydrogel size was not stated in the experimental study.

The final computed cumulative release percent for both oxygen and VEGF agreed with the final release percent of the experiments. Despite a slight overestimation in both computations before 40 hours, the general trends of oxygen and VEGF diffusivity matched with the experimental results.

4.5 Effects of Varying Hydrogel Concentration

The goal of the hydrogel injection was to regenerate healthy tissue before significant scarring occurred. Multiple trials testing different hydrogel concentrations were performed to determine the optimal initial concentrations of O_2 and VEGF needed in the hydrogel to reach therapeutic levels. Various initial concentrations of O_2 and VEGF were loaded into the hydrogel, and the computation was run. For each test, the average concentration of O_2 or VEGF across all the mesh points within the damaged tissue domain was calculated. Figure 10 shows the plots of concentration as a function of time for both oxygen and VEGF; the specific concentration that produced the highest average was chosen.

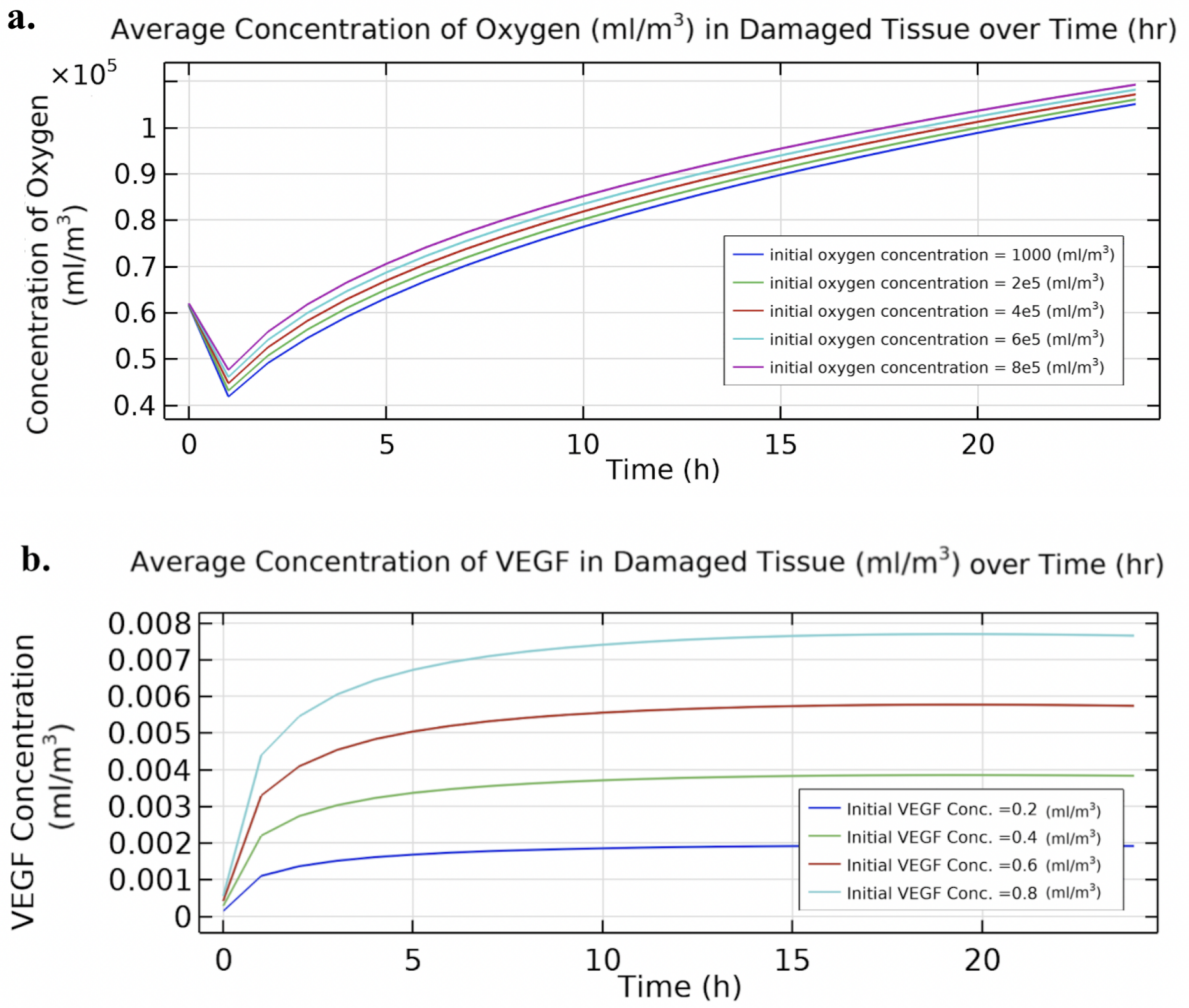

Fig 10. Varying Initial Concentrations of Diffusants within Hydrogel. a) Various initial hydrogel concentrations of O_2 and average concentrations of O_2 they produced in the damaged tissue over 24 hours. b) Various initial hydrogel concentrations of VEGF and the average concentrations of VEGF they produce in the damaged tissue over 24 hours.

Based on Figure 10a, 8×10^5 ml/m^3 was chosen as the initial hydrogel concentration since it resulted in the smallest initial dip in oxygen concentration. Large initial dips, which represented sub-therapeutic oxygen levels, should have been minimized. As shown in Figure 10b, an initial value of 0.8 ml/m^3 delivered the most VEGF to the damaged tissue.

4.6 Sensitivity Analysis

As seen in Figure 10, several parameters were varied based on the maximum and minimum literature value found, and the corresponding final concentrations of oxygen and VEGF in the damaged tissue were measured.

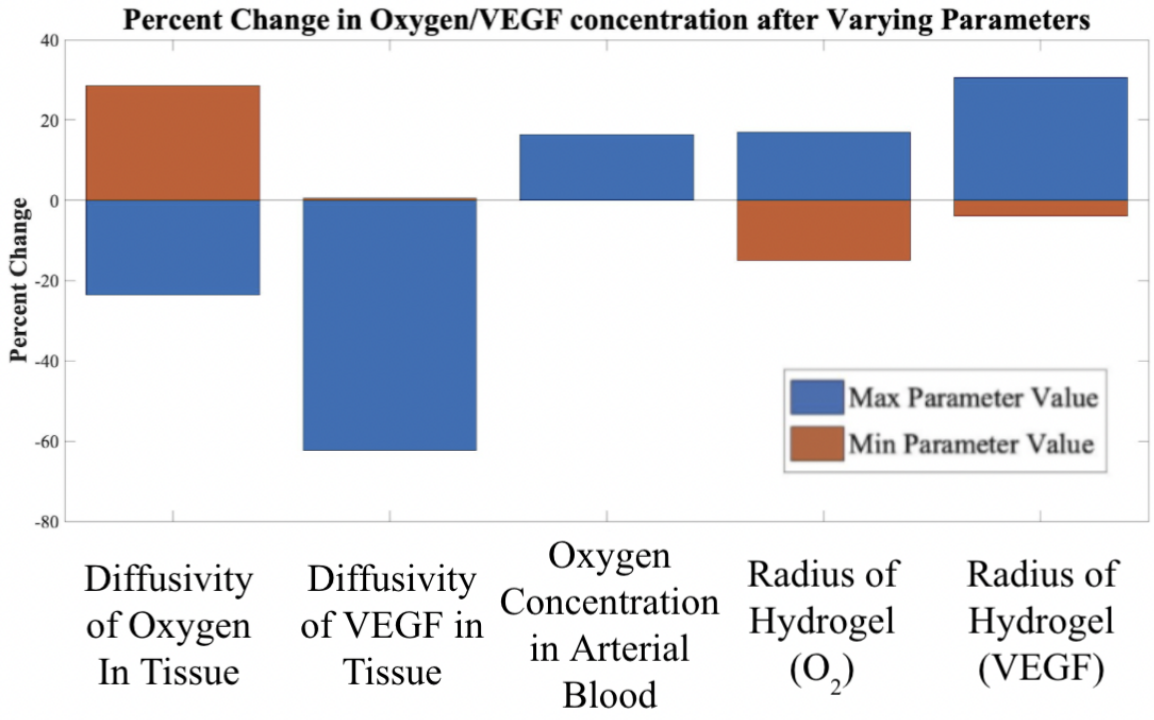

Fig. 10. Percent change in oxygen/VEGF concentration after varying 5 parameters. Maximum and minimum values for each parameter are found in Appendix 7.D, except for the hydrogel radius, which was varied by $\pm$ 10%. Note that the model used the minimum value of oxygen concentration in arterial blood.

Figure 10 illustrates that the diffusivity of VEGF in tissue was the most sensitive parameter because it caused the most variability in average therapeutic agent concentration within the damaged tissue at 24 hours. VEGF diffusivity may be the most sensitive since it had the widest range of values in literature: from 10^{-8} m^2/s to 10^{-11} m^2/s. When the VEGF diffusivity was increased by 8750% , the percent change in the concentration of VEGF in the damaged tissue at 24 hours compared to the original model (diffusivity of $1.3 \times 10^{-10} m^2/s$) was about -62%. Decreasing the diffusivity did not make a significant difference in VEGF concentration. Therefore, there would be a large error in the computed concentration if the experimental diffusivity of VEGF in the tissue was greater than the value used in this model.

The percentage change in oxygen and VEGF concentrations in damaged tissue after varying hydrogel diffusivity parameters was shown in Figure 11. Changing diffusivity of oxygen in tissue also resulted in a large variation in the amount of oxygen in the tissue at 24 hours. Both decreasing and increasing diffusivity greatly impacted the final concentration. Oxygen concentration in arterial blood and radius of the hydrogel were also varied based on the literature values. Increasing both these parameters caused the final concentration to increase +18%.

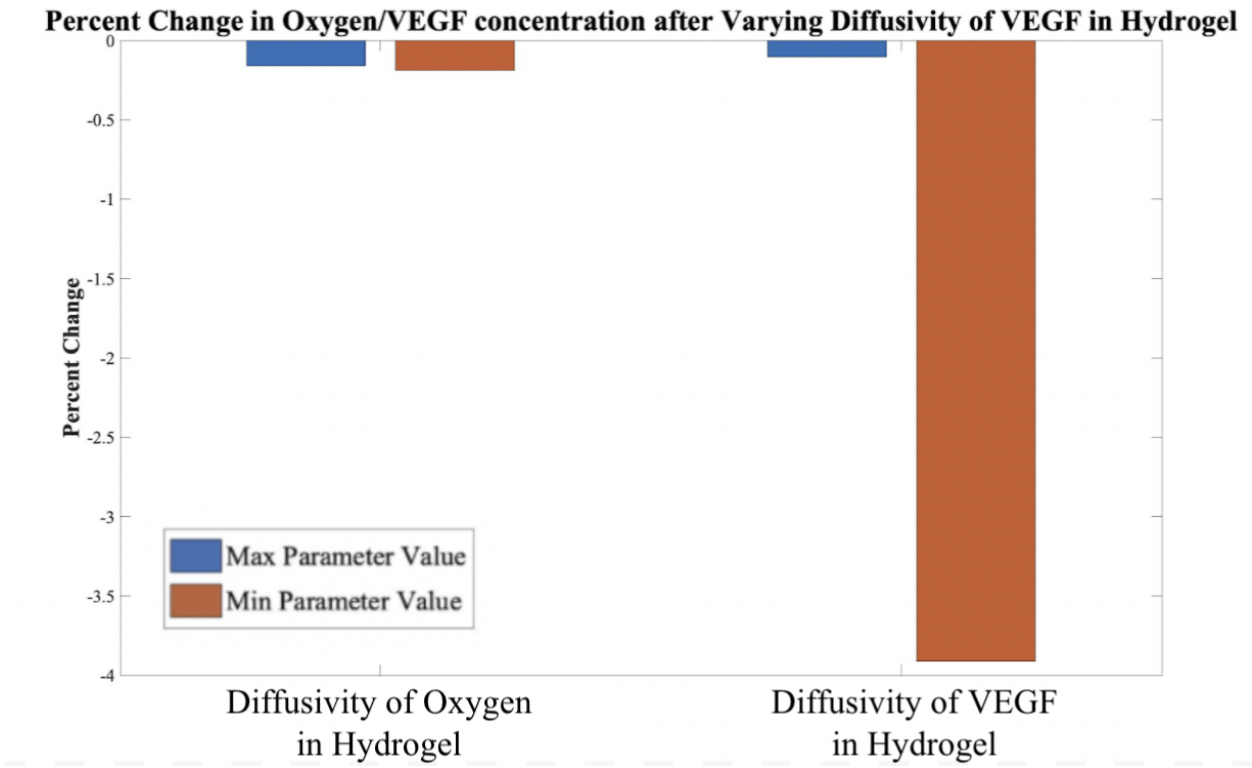

Fig 11. Percent change in oxygen/VEGF concentration after varying diffusivity in hydrogel. The percent change of oxygen concentration in damaged tissue at 24 hours was calculated to be -0.16% and -0.19% for a +5.2% and -4.94% change in oxygen diffusivity in hydrogel, respectively. The change in VEGF concentration was -0.10% and -3.9% for a +21,900% and -97.9% change in VEGF diffusivity in hydrogel, respectively.

As seen in Figure 11, varying the hydrogel diffusivities caused a minimal change of less than -0.25% in the oxygen and VEGF concentrations in damaged tissue. Consequently, these parameters were not sensitive within the model.

To determine the most sensitive parameter, the parameters were all varied by +10% and -10% as seen in Figure 12, and the final average concentration in the damaged tissue was determined.

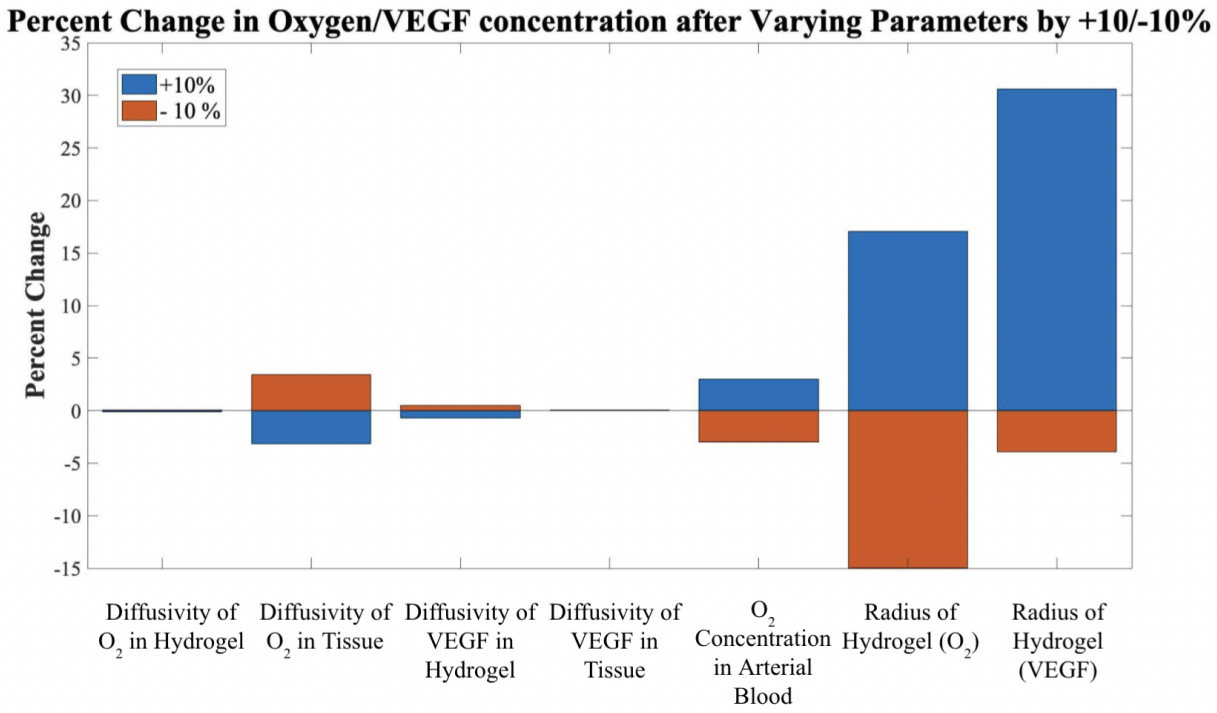

Fig 12. Percent change in oxygen/VEGF concentration after varying parameters by ±10%. The greatest change, +30%, occurred when changing the radius of hydrogel. Diffusivity of VEGF in tissue was the least sensitive parameter, with <1% changes in VEGF concentration.

It was determined that the parameter with the least sensitivity to testing was the diffusivity of VEGF in tissue. As shown in Figure 12, the VEGF diffusivity range from -0.72% to 0.49% was minimal compared to the other groups. In contrast, the concentration of oxygen and VEGF were the most sensitive to fluctuations in hydrogel radius. Varying the radius by +10% increased oxygen concentration by +17% and VEGF concentration by +30%. However, shrinking the radius -10% decreased the VEGF concentration by less than 5%. Since the sensitivity analysis was based on the final VEGF concentration (at 24 hours) in the damaged tissue rather than the average concentration throughout the 24 hours, it provides a snapshot in time of how much oxygen and VEGF had been released from the hydrogel. Therefore, the results are dependent upon time of peak concentration. Increasing the radius by +10% considerably increased the release rate of VEGF, resulting in the large 30% increase in VEGF concentration since the time of peak concentration greatly differed from that of the original hydrogel. The smaller hydrogel had a VEGF release rate more similar to that of the original hydrogel size, so the concentration at 24 hours did not appreciably change. This sensitivity analysis shows that radius size should play a large role in design considerations as it can influence drug release rates and peak concentration times.

5.0 Conclusion

5.1 Summary of Results

Immediately following myocardial infarction, oxygen and VEGF levels in the damaged heart tissue are depleted. If this condition is left untreated, cardiac tissue would permanently weaken. In this study, delivery of oxygen and VEGF to damaged heart tissue via an injectable hydrogel was modeled. This device was designed to deliver sufficient oxygen and VEGF to the entire wounded region of the heart tissue – 3.50 cm in length by 1.50 cm in height. A target oxygen concentration of 7.58×10^4 ml O_2/m^3 tissue was required in the infarcted tissue region to return tissue oxygen levels to normal. The model determined the time to deliver the minimum effective concentration of oxygen throughout the wounded region to be 22 hours after injection of the hydrogel. Similarly, the time for VEGF to diffuse and reach all cells of the wounded tissue with a concentration above 0.001 ml/m^3 was evaluated to be 22 hours. After 24 hours, the concentration increased to 0.00137 ml/m^3. In order to reach these desired levels across the entire wounded region, the hydrogel must be manufactured to hold an initial concentration of 8×10^5 ml/m^3 O_2 and 0.8 ml/m^3 VEGF.

5.2 Research Limitations

While computational modeling provides several benefits compared to *in vivo* testing, there are also limitations. First, discretization of data from an analytical solution always retains some amount of error, but this was mitigated with an increasing number of computations. Conducting a mesh converge and time step convergence for modeling helped decrease the discretization error, but did not completely eliminate it. The limitations specific to this study primarily come from the simplifications made to the setting. A real heart ventricle is not perfectly rectangular, and infarcted tissue will form in irregular shapes. There is no clear boundary between damaged and healthy tissue like in this experiment. In cases where the geometry of damaged tissue is extremely different from the model geometry, there will be significant differences between the computational and experimental results. The boundary conditions, reaction rates and assumptions related to the parameter values used in this experiment also have limitations. For example, differences in diffusivities between healthy and damaged tissue were ignored. Likewise, a constant blood flow was set as the convective boundary condition, whereas in reality, blood ebbs and flows with the rhythmic pumping of the heart. These simplifications were made only after confirming that they did not grossly change the nature of the computation, but they should be acknowledged when using this study for future research.

5.3 Design Recommendations

The hydrogel was determined to provide an effective concentration of oxygen throughout the entire wounded tissue by 22 hours. The VEGF took approximately 2 hours longer to reach the entirety of the wounded tissue. Since both therapeutic agents were delivered before the time for

sufficient scar tissue to form, 3 weeks, an oxygen- and VEGF-releasing hydrogel showed promise as a viable technology in preventing scar tissue formation. The highest therapeutic results will occur if injected immediately following a heart attack. The concentration of VEGF takes a slightly longer time to diffuse, but was still successful in accelerating tissue regeneration, which takes a much larger time of at least 3 weeks to fully replace infarcted cardiac myocytes. The selected hydrogel radius of 2.59×10^{-3}m and initial concentrations were optimized to fit a predetermined size of damaged tissue. For *in vivo* scenarios, the size of the damaged or infected tissue will vary from the model's determined dimensions, so the actual hydrogel size for injection must be scaled to the patient's infarct size. As determined by the positive correlation between hydrogel radius and release percentage in the sensitivity analysis, a larger infarcted tissue area requires a larger volume hydrogel, and vice versa.

This experiment modeled the hydrogel's location equidistant from the inner and outer walls of the ventricle. However, the mass transfer profile of oxygen over the course of 24 hours showed a significantly higher delivery to the inner region of the ventricle (Figure 7). This is a result of the bloodstream delivering another source of oxygen from the inner wall via convection. While oxygen reached a therapeutic level throughout the damaged tissue, it should be noted that the benefit of the hydrogel will improve if injected closer to the surface of the ventricle wall, about ⅓ of the distance from the surface to the ventricle. The diffusion effect combined with the convective boundary would deliver oxygen from both sides of the heart wall, reducing the overlap in diffusion and decreasing the time for the damaged tissue to recover to the necessary oxygen level. To the extent possible, if injecting multiple hydrogels instead of scaling the size, the user should try to inject hydrogels with a radius of 2.88 cm approximately 3.5–4.0 cm apart near the outer layer of the ventricle; this will maximize the volume covered and ideally minimize overlap.

While fibrin is a well-researched biomaterial, creating a hydrogel that reliably swells to a constant radius may be challenging. To ensure that the hydrogels for each treatment have similar material properties and swelling/deswelling kinetics, the manufacturing process would need to be precise and robust. Because of the need for stringent quality control, the hydrogel may be expensive to manufacture in bulk.

5.4. Future Research

Future research in this field can take steps to improve the delivery mechanism of the hydrogel. If the surface of the ventricle requires the most oxygen, then it is possible that a flat hydrogel scaffold over the ventricle may be able to deliver therapeutic agents more efficiently than a spherical form. The time between heart attack and hydrogel injection is also highly variable. Differences in ambulance transport time, availability of ER hospital beds, and awareness that a heart attack has occurred all contribute to the amount of tissue damage before injection. Further research needs to be done on the average time until treatment is sought in order to better understand how much tissue needs to be healed, and subsequently, if this hydrogel device is a viable option for treatment.

Fortunately, this hydrogel is very sensitive to radius, so if a large volume needs to be treated, increasing the hydrogel size by just a few millimeters will significantly increase diffusion distance. Another step that can be taken for future studies is changing the contents delivered from the hydrogel, such as by using stem cells in lieu of VEGF and analyzing its comparative effect on tissue regeneration.

6.0 Acknowledgements

We would like to thank Professor Ashim Datta and Kalayarasan Seranthian in the Department of Biological and Environmental Engineering at Cornell University, without whom this work would not have been possible. In addition, we extend our gratitude to Dr. Rick Evans for his guidance and direction in the writing of this paper.

7.0 Appendix

7.A Parameters

Parameter	Value	Units	Source
Hydrogel Radius	Initial radius - 0.0028 m (Dependent on time)	m	[17]
Damaged Tissue Size	0.025 x 0.015 m	m	[18]
Healthy Tissue Size	0.04 x 0.015 m	m	[18]
Diffusion Coefficient of oxygen through Hydrogel	$1.7 \times 10^{-9} m^2/s$	m^2/s	[19]
Diffusion Coefficient of VEGF through Hydrogel	$1 \times 10^{-9} m^2/s$	m^2/s	[20]
Initial concentration of oxygen in hydrogel	User input - 8×10^5	ml/m^3	Not Applicable
Initial concentration of VEGF in hydrogel	User input - 0.8	ml/m^3	Not Applicable
Diffusivity of oxygen through cardiac tissue	0.3x 10^{-9}	m^2/s	[21]
Diffusivity of VEGF through cardiac tissue	1.13 x 10^{-10}	m^2/s	[22]
Initial concentration of oxygen in damaged tissue	6.06 x 10^4	ml O_2/m^3	[23], [24]
Initial concentration of VEGF in damaged tissue	0	n/a	[25]
Initial concentration of oxygen in healthy tissue	7.58 x 10^4	ml O_2/m^3	[24]
Initial concentration of VEGF in healthy tissue	0	ml /m^3	[25]
Concentration of oxygen in blood	2 x 10^5	mlO_2/m^3	[24]
Concentration of VEGF in blood	0	n/a	[25]
Consumption rate of oxygen by tissue	18 x 10^{-3}	mol/(m^3·s)	[26]
Consumption rate of oxygen by unhealthy tissue	0.17 ml/g/beat → 1231.25 ml/m^3/s	ml/m^3/s	[27]
Degradation rate of VEGF outside the cell	2.5 x 10^{-4} s^{-1} ($\tau_{1/2}$ ~ 40 min)	s^{-1}	[28]
Hydrogel deswelling rate constant	k = 8.0225368 x 10-6 s^{-1}	s^{-1}	[16]

7.B CPU and Memory Use

```
Time-stepping completed.
Solution time: 134 s. (2 minutes, 14 seconds)
Physical memory: 10.89 GB
Virtual memory: 15.83 GB
Ended at May 11, 2021 2:00:36 PM.
----- Time-Dependent Solver 1 in Study 1/Solution 1 (sol1) ---------------------->
================================================================================
```

7.C Hydrogel Deswelling

Once the hydrogel is injected into the damaged heart tissue, it will deswell over time, and the radius will decrease. However, this does not occur at a constant rate. Hydrogel deswelling kinetics can be very difficult to model, as this will depend on the molecular chain length of the hydrogel monomers, polymer network density, temperature, pH, solvent, etc [15]. From research that has been done on general hydrogel swelling and deswelling kinetics [16], an exponential decay function would best capture the change in radius of the hydrogel over time. Since the material properties of the hydrogel do not change with time, this function can be compared to the initial volume of the hydrogel with the volume of the hydrogel at any given time.

$$V_{final} = V_{initial} \cdot e^{-kt}$$

Using biomaterial design techniques, the hydrogel can be tuned to fit the experiment. The hydrogel sphere was designed to shrink to half of the original size over the course of 24 hours. With this knowledge, the deswelling rate constant was found.

$$V_{final} = \frac{1}{2} \cdot V_{initial};\ t = 24\ hours\ (86400\ seconds)$$
$$\frac{1}{2} = e^{-k \cdot 86400\ [s]}$$
$$k = 8.0225368 \times 10^{-6}\ [s^{-1}]$$

Upon finding *k*, the equation can be modified to find the rate of change of the radius. Below, R_i was a constant corresponding to the initial radius of the hydrogel sphere, and R_f was the radius of the hydrogel sphere at time *t*.

$$V_f = V_i \cdot e^{-kt},\ where\ V = \frac{4}{3}\pi R^3$$
$$\frac{4}{3}\pi {R_f}^3 = \frac{4}{3}\pi {R_i}^3 \cdot e^{-kt}$$
$$R_f^{\ 3} = R_i^{\ 3} \cdot e^{-kt}$$
$$R_f = R_i \cdot e^{-kt/3}$$

$$\frac{dR_f}{dt} = R_i \cdot e^{-kt/3} \cdot (-k/3)$$

$$\frac{dR_f}{dt} = v = \frac{-R_i \cdot k}{3} \cdot e^{\frac{-k \cdot t}{3}}$$

Now, substituting in the numerical values for R_i and k, this equation can be plugged into v for the Prescribed Normal Mesh Velocity in the Deformed Geometry physics. When the model was run, the radius of the hydrogel boundary decreased quickly at early times, and the velocity slowed down over time. Eventually, the volume of the hydrogel after 24 hours was about half of its initial volume.

7.D Sensitivity Analysis Literature Values

Parameter	Current Model Value	Literature Maximum Value	Literature Minimum Value	Max Percent Change (%)	Min Percent Change (%)
Diffusivity of Oxygen in tissue (m^2/s)	0.3 x 10^{-9} [21]	1.5 × 10^{-9} [29]	6 x 10^{-11} [30]	400	-80
Diffusivity of Oxygen in hydrogel (m^2/s)	1.7 x 10^{-9} [19]	1.784 x 10^{-9} [31]	1.616 x 10^{-9} [31]	5.20	-4.94
Diffusivity of VEGF in tissue (m^2/s)	1.13 x 10^{-10} [22]	10^{-8} [32]	10^{-11} [32]	8749.56	-91.15
Diffusivity of VEGF in hydrogel (m^2/s)	1 x 10^{-9} [20]	2.2 ± 0.3 × 10^{-7} [20]	2.1 x 10^{-11} [20]	21900	-97.9
Initial Radius of Hydrogel *(m)*	0.002879 [17]	0.0031669	0.0025911	10	-10
Amount of O_2 in convective boundary layer (bloodstream) $(ml/m^3\ blood)$	2 x 10^5 [24]	3.1 x 10^5 [33]	2 x 10^5 [33]	55	0

7.E Concentration of Oxygen/VEGF based on Literature Values in 7.D

	Amount of oxygen/VEGF in damaged tissue at 24 hours (ml/m^3)				
Parameter Varied	Results Based on Current Model Value	Results Based on Maximum Value	Results Based on Minimum Value	Max % Change in Results	Min % Change in Results
Diffusivity of oxygen in tissue	257234.4831	330974.5913	196878.2545	-30.65662521	28.66649423
Diffusivity of	257234.4831	256745.2337	256819.1262	-0.1617312957	-0.1901958855

oxygen in hydrogel					
Diffusivity of VEGF in tissue	0.0105083742	0.01056659642	0.003955840363	-165.6420187	0.5540555024
Diffusivity of VEGF in hydrogel	0.01050837093	0.01009740079	0.01049752708	-0.1032990615	-3.910883451
Initial Radius of hydrogel (VEGF)	0.01050837093	0.01009740159	0.01372620929	30.62166703	-3.910875812
Initial Radius of hydrogel (Oxygen)	301100.2295	218745.7398	257234.4831	17.05282509	-14.96251313
Amount of O_2 in convective boundary layer (bloodstream)	257234.4831	257234.4831	299537.1942	14.12269058	0

8.0 References

[1] C. D. Fryar, T. C. Chen, and X. Li, “Prevalence of uncontrolled risk factors for cardiovascular disease: United States, 1999-2010.,” NCHS Data Brief, no. 103, pp. 1–8, 2012.

[2] “What Is a Heart Attack?” *heart.org*, American Heart Association, Jul. 31, 2016. [Online]. Available: www.heart.org/en/health-topics/heart-attack/about-heart-attacks. [Accessed May 1, 2021].

[3] T. Yokota, J. McCourt, F. Ma, M. Seldin, A. J. Lusis, A. Deb, “Type V Collagen in Scar Tissue Regulates the Size of Scar after Heart Injury,” Cell, vol. 182, no. 3, pp. 545-562.e23, 2020.

[4] M. Gholipourmalekabadi, S. Zhao, B. S. Harrison, M. Mozafari, and A. M. Seifalian, “Oxygen-Generating Biomaterials: A New, Viable Paradigm for Tissue Engineering?,” Trends Biotechnol., vol. 34, no. 12, pp. 1010–1021, 2016.

[5] L. L. Y. Chiu, M. Radisic, and G. Vunjak-Novakovic, “Bioactive Scaffolds for Engineering Vascularized Cardiac Tissues,” Macromol. Biosci., vol. 10, no. 11, pp. 1286–1301, 2010.

[6] “Entering a new era in vascular and cardiac regeneration research.” astrazeneca.com, 2021. [Online]. Available: https://www.astrazeneca.com/what-science-can-do/topics/next-generation-therapeutics/entering-a-new-era-in-vascular-and-cardiac-regeneration-research.html. [Accessed May 1, 2021].

[7] J. Zhu and R. E. Marchant, “Design properties of hydrogel tissue-engineering scaffolds,” Expert Rev. Med. Devices, vol. 8, no. 5, pp. 607–626, 2011.

[8] A. M. Prabhat, M. L. Kuppusamy, S. K. Naidu, S. Meduru, P. T. Reddy, A. Dominic, M. Khan, B. K. Rivera, P. Kuppusamy, “Supplemental Oxygen Protects Heart Against Acute Myocardial Infarction,” Front. Cardiovasc. Med., vol. 5, no. August, pp. 1–10, 2018.

[9] B. Berman. “Our Bodies’ Velocities, By the Numbers.” *discovermagazine.com*, Jun. 3, 2014. [Online]. Available: https://www.discovermagazine.com/mind/our-bodies-velocities-by-the-numbers. [Accessed May 1, 2021].

[10] M. K. Gupta, J. R. Martin, T. A. Werfel, T. Shen, J. M. Page, and C. L. Duvall, “Cell protective, ABC triblock polymer-based thermoresponsive hydrogels with ROS-triggered degradation and drug release,” J. Am. Chem. Soc., vol. 136, no. 42, pp. 14896–14902, 2014.

[11] O. Yargi, S. Ugur, and O. Pekcan, “Diffusion energies of oxygen diffusing into polystyrene (PS)/poly (N-isopropylacrylamide) composites,” Polym. Adv. Technol., vol. 23, no. 4, pp. 776–782, 2012.

[12] R. J. McMurtrey, “Analytic models of oxygen and nutrient diffusion, metabolism dynamics, and architecture optimization in three-dimensional tissue constructs with applications and insights in cerebral organoids,” Tissue Eng. - Part C Methods, vol. 22, no. 3, pp. 221–249, 2016.

[13] L. Ouyang, Y. Dan, Z. Shao, S. Yang, C. Yang, G. Liu, D. Duan, “MMP‑sensitive PEG hydrogel modified with RGD promotes bFGF, VEGF and EPC‑mediated angiogenesis,” Exp. Ther. Med., pp. 2933–2941, 2019.

[14] Y. D. P. Limasale, P. Atallah, C. Werner, U. Freudenberg, and R. Zimmermann, “Tuning the Local Availability of VEGF within Glycosaminoglycan-Based Hydrogels to Modulate Vascular Endothelial Cell Morphogenesis,” Adv. Funct. Mater., vol. 30, no. 44, 2020.

[15] R. Ebrahimi, “The study of factors affecting the swelling of ultrasound-prepared hydrogel,” Polym. Bull., vol. 76, no. 2, pp. 1023–1039, 2019.

[16] E. S. Gil and S. M. Hudson, “Effect of silk fibroin interpenetrating networks on swelling/deswelling kinetics and rheological properties of poly(N-isopropylacrylamide) hydrogels,” Biomacromolecules, vol. 8, no. 1, pp. 258–264, 2007.

[17] A. H. Zisch, M. P. Lutolf, M. Ehrbar, G. P. Raeber, S. C. Rizzi, N. Davies, H. Schmökel, D. Bezuidenhout, V. Djonov, P. Zilla, J. A. Hubbell, “Cell‑demanded release of VEGF from synthetic, biointeractive cell‑ingrowth matrices for vascularized tissue growth,” FASEB J., vol. 17, no. 15, pp. 2260–2262, 2003.

[18] S. Mohammadi, A. Hedjazi, M. Sajjadian, N. Ghoroubi, M. Mohammadi, and S. Erfani, “Study of the normal heart size in Northwest part of Iranian population: a cadaveric study,” J. Cardiovasc. Thorac. Res., vol. 8, no. 3, pp. 119–125, 2016.

[19] L. Figueiredo et al., “Assessing glucose and oxygen diffusion in hydrogels for the rational design of 3D stem cell scaffolds in regenerative medicine,” J. Tissue Eng. Regen. Med., vol. 12, no. 5, pp. 1238–1246, 2018.

[20] L. Abune, N. Zhao, J. Lai, B. Peterson, S. Szczęsny, Y. Wang, “Macroporous Hydrogels for Stable Sequestration and Sustained Release of Vascular Endothelial Growth Factor and Basic Fibroblast Growth Factor Using Nucleic Acid Aptamers,” ACS Biomater Sci Eng., vol. 5, no. 5, pp. 2382–2390, 2019.

[21] D. A. Brown, W. R. MacLellan, H. Laks, J. C. Y. Dunn, B. M. Wu, R. E. Beygui. “Analysis of Oxygen Transport in a Diffusion-Limited Model of Engineered Heart Tissue,” Biotechnol. Bioeng., vol. 97, no. 4, pp. 962–975, 2007.

[22] F. Mac Gabhann, J. W. Ji, and A. S. Popel, “Computational model of vascular endothelial growth factor spatial distribution in muscle and pro-angiogenic cell therapy,” PLoS Comput. Biol., vol. 2, no. 9, pp. 1107–1120, 2006.

[23] B. H. Davis, Y. Morimoto, C. Sample, K. Olbrich, H. A. Leddy, F. Guilak, D. A. Taylor, “Effects of myocardial infarction on the distribution and transport of nutrients and oxygen in porcine myocardium,” J. Biomech. Eng., vol. 134, no. 10, pp. 1–6, 2012.

[24] “Coronary Oxygen Delivery to the Myocardium.” *cvphysiology.com,* Sep. 28, 2011. [Online]. Available: https://www.cvphysiology.com/CAD/CAD002#:~:text=The%20normal%20oxygen%20concentration%20in,O2%2Fmin%20per%20100g.

[25] C. Kut, F. Mac Gabhann, and A. S. Popel, “Where is VEGF in the body? A meta-analysis of VEGF distribution in cancer,” Br. J. Cancer, vol. 97, no. 7, pp. 978–985, 2007.

[26] M. Radisic, W. Deen, R. Langer, and G. Vunjak-Novakovic, “Mathematical model of oxygen distribution in engineered cardiac tissue with parallel channel array perfused with culture medium containing oxygen carriers,” Am. J. Physiol. - Hear. Circ. Physiol., vol. 288, no. 3 57-3, pp. 1278–1289, 2005.

[27] H. Laine, C. Katoh, M. Luotolahti, H. Yki-Järvinen, I. Kantola, A. Jula, T. O. Takala, U. Ruotsalainen, H. Iida, M. Haaparanta, P. Nuutila, J. Knuuti, “Myocardial oxygen consumption is unchanged but efficiency is reduced in patients with essential hypertension and left ventricular hypertrophy,” Circulation, vol. 100, no. 24, pp. 2425–2430, 1999.

[28] P. Vempati, A. S. Popel, F. M. Gabhann. “Extracellular regulation of VEGF: isoforms, proteolysis, and vascular patterning,” Cytokine Growth Factor Rev, vol. 25, no. 1, pp. 1–19, 2014.

[29] W. L. Rumsey, C. Schlosser, E. M. Nuutinen, M. Robiolio, and D. F. Wilson, “Cellular energetics and the oxygen dependence of respiration in cardiac myocytes isolated from adult rat,” J. Biol. Chem., vol. 265, no. 26, pp. 15392–15399, 1990.

[30] J. D. B. Macdougall and M. Mccabe, “Diffusion coefficient of oxygen through tissues,” Nature, vol. 215, no. 5106, pp. 1173–1174, 1967.

[31] S. M. Ehsan and S. C. George, “Nonsteady state oxygen transport in engineered tissue: Implications for design,” Tissue Eng. - Part A, vol. 19, no. 11–12, pp. 1433–1442, 2013.

[32] R. J. McMurtrey, “Roles of Diffusion Dynamics in Stem Cell Signaling and Three-Dimensional Tissue Development,” Stem Cells Dev., vol. 26, no. 18, pp. 1293–1303, 2017.

[33] J. Shaikh. “What Are Blood Oxygen Levels? Chart.” *medicinenet.com,* Oct. 15, 2020. [Online]. Available: https://www.medicinenet.com/what_are_blood_oxygen_levels/article.htm.